

Dynamics of the seasonal variations in the Indian Ocean from TOPEX / POSEIDON sea surface height and an ocean model

Jiayan Yang

Woods Hole Oceanographic Institution, Woods Hole, Massachusetts

Lisan Yu

University of Maryland, College Park, Maryland

Chester J. Koblinsky and David Adamec

Goddard Space Flight Center, NASA, Greenbelt, Maryland

Abstract. Observations from the TOPEX / POSEIDON (T/P) altimeter reveal that the sea level in the Indian Ocean varies strongly with season. Surface undulations propagate eastward along the equator and westward outside the equatorial waveguide. The forcing mechanisms responsible for such variations are investigated in this paper by analyzing T/P data and surface wind-stress forcing, and by using a nonlinear, 2.5-layer, reduced gravity model. Both the data and the model show that Kelvin and Rossby waves forced by the Indian Ocean monsoon are primarily responsible for the seasonal sea-level change in the tropical and the subtropical Indian Ocean.

1. Introduction

The wind-driven circulation in the Indian Ocean has great seasonal variation due to monsoon forcing. There have been many studies of the seasonal circulation in the Indian Ocean [e.g., *Lighthill*, 1969; *Luther and O'Brien*, 1985, 1989; *McCreary et al.*, 1993; *Jensen*, 1993; *Perigaud and Delecluse*, 1992; *Clarke and Liu*, 1993] in which the roles of Kelvin and Rossby waves have been greatly emphasized. These waves can propagate over great distances and affect ocean circulation in remote regions far from their origin [e.g., *Adamec and O'Brien*, 1978]. *Yu et al.* [1991] and *Potemra et al.* [1991] applied this "teleconnection mechanism" to the Indian Ocean and proposed that equatorial Kelvin waves contribute significantly to the seasonal gyre circulation in the Bay of Bengal through reflected Rossby waves. This mechanism remains to be examined by using observations. Sea surface height (SSH) data from the T/P altimeter are ideal for this purpose because of their basin-wide coverage. The main objective of this paper is to use this data set, combined with an ocean model, to investigate the main forcing mechanisms in the tropical and subtropical Indian Ocean.

2. Model Formulation

The ocean model used in this study is a nonlinear, 2.5-layer, reduced gravity model formulated in spherical coordinates. It is forced by the climatological wind stress data from Florida State University [*Stricherz et al.*, 1993]. The initial layer thicknesses are 200 m and 250 m for H_1 and H_2 respectively. The potential density in each layer is estimated from the basin-wide and annually averaged data from *Levitus et al.* [1994], yielding 1024.040, 1026.576, and 1027.530 kg m^{-3} for each of the three layers. The phase speeds of the first and second baroclinic mode Kelvin waves, computed following *McCreary et al.* [1993], are 2.76 m s^{-1} and 1.23 m s^{-1} , respectively. The viscosity is 1500 $\text{m}^2 \text{s}^{-1}$. The model includes the same entrainment parameterization as *Jensen* [1991]. The model is spun up for 50 years to achieve a steady seasonal cycle. The result used in this paper is from the 50th year. The boundary conditions are no normal flow except at the southern boundary where an open boundary condition is used. The model's horizontal resolution is $1^\circ \times 1^\circ$ and the Arakawa C-grid is used.

3. Discussion

During the northeast monsoon season in the northern winter, the zonal wind is westward at the equator, so it forces upwelling Kelvin waves and downwelling Rossby waves in the equatorial waveguide. Figure 1a shows that the SSH deviation is negative in the equatorial and eastern basins in January. Two months later in March, the wave signals become even clearer (Figure 1b). Upwelling Rossby waves are radiated offshore from the eastern boundary. Meanwhile, downwelling Rossby waves generated by the easterly wind component in the equatorial ocean are clearly shown near the western boundary (Figure 1b). To illustrate this wave-generation mechanism, the evolution of wind stress along the equator and that along the eastern boundary are presented in Figures 2a and b. The easterly wind dominates at the equator between January and April (Figure 2a), and it is responsible for the generation of

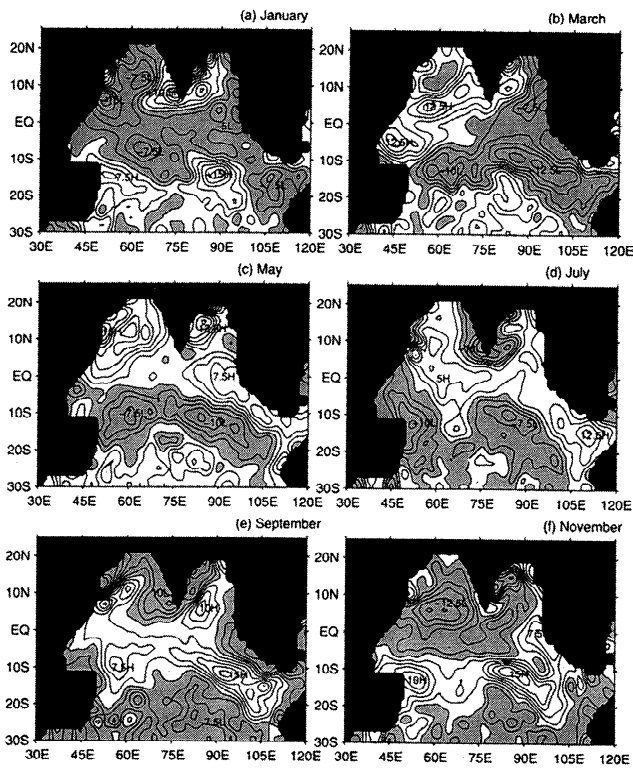


Figure 1. Seasonal deviations of the SSH in TOPEX / POSEIDON observations. (Contour interval: 2.5 cm; negative SSH deviations are shaded).

upwelling Kelvin waves in the eastern and downwelling Rossby waves in the western equatorial basin.

Rossby waves near the eastern boundary can be generated either locally by alongshore winds or remotely by reflection of equatorial Kelvin waves. North of the Indonesian Throughflow (ITF), roughly between 12°S and 21°S, the alongshore wind component in the northern winter is southward (Figure 2b), so it forces upwelling Rossby waves in the northern hemisphere and downwelling Rossby waves in the southern hemisphere.

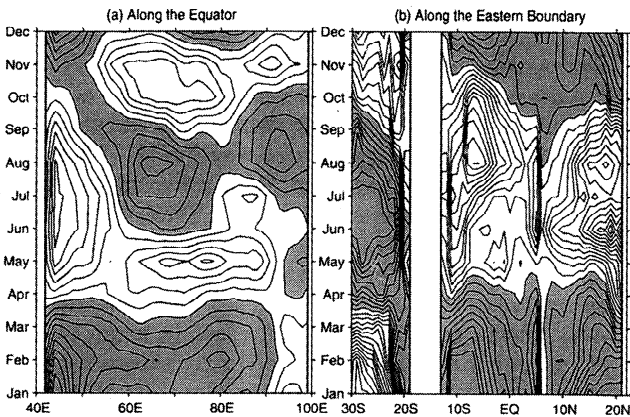


Figure 2. Time series of the FSU pseudo wind stress ($\vec{U}|U|$, where \vec{U} is wind speed vector), (a) zonal component along the equator, and (b) along coast component at the eastern boundary. (Contour interval: $3 \text{ m}^2 \text{ s}^{-2}$; easterly wind in (a) and northerly wind in (b) are shaded).

This indicates that, while upwelling Rossby waves in the eastern Bay of Bengal can be attributed to either the local or the remote mechanisms, those in the southeastern Indian Ocean, between the equator and the ITF, can only be forced by a remote mechanism since alongshore wind produces downwelling waves. South of the ITF the alongshore wind has an opposite seasonal cycle, i.e., it is directed northward in the northern winter. Thus it forces upwelling Rossby waves locally. In fact, upwelling waves off the Australian coast in January (Figure 1a) were likely generated by the alongshore wind.

Positive SSH deviations are found in regions off both coasts of India in the northern winter (Figure 1a–b). These downwelling Rossby waves were generated in the previous southwest monsoon season. The wind along the west coast of India is southward during the northern winter, so it forces upwelling Rossby waves. Therefore the downwelling Rossby waves in the eastern Arabian Sea are not generated locally.

The southwest monsoon starts to develop in April (Figure 2a), and downwelling equatorial Kelvin waves are excited. Indeed the SSH deviation in May (Figure 1c) shows that downwelling Kelvin waves with the elevated SSH have already reached the eastern boundary, and downwelling Rossby waves are just being radiated offshore. Meanwhile upwelling Rossby waves, generated in the previous northeast monsoon, still dominate to the west of those newly radiated downwelling Rossby waves. The alongshore wind at the eastern boundary north of the ITF, between April and September, is mostly northward. This will force upwelling (downwelling) Rossby waves in the southern (northern) hemisphere. Therefore the downwelling Rossby

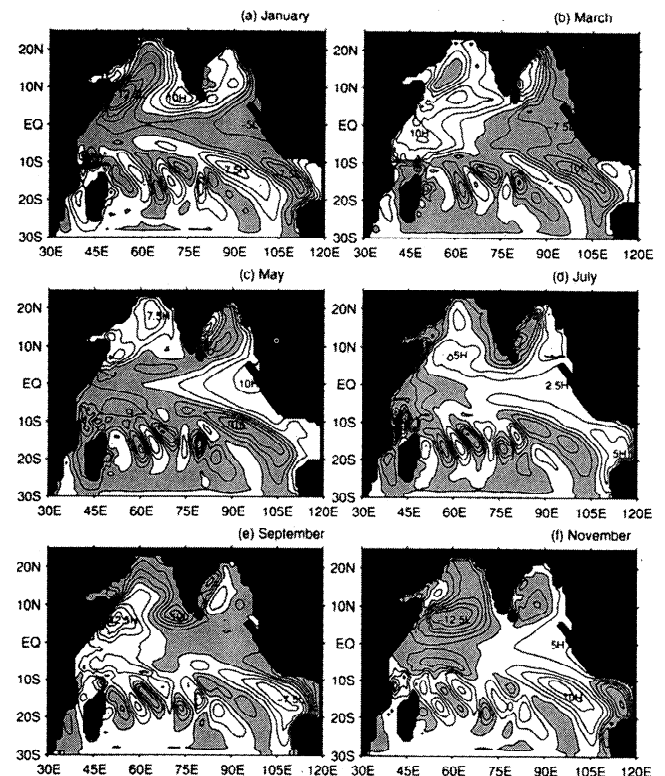


Figure 3. Same as Figure 1 except from our numerical model.

waves observed in the southern Indian Ocean off the eastern boundary between the equator and the ITF in late spring and early summer (Figure 1c–d for May and July) could not be generated locally by alongshore wind stress. They must originate from equatorial Kelvin waves.

Figure 2a reveals an interesting feature for the zonal wind along the equator. While the annual cycle dominates in the western basin, the semi-annual cycle is more remarkable in the central and eastern basins. Therefore both annual and semi-annual Kelvin and Rossby waves are forced in the equatorial waveguide. Indeed upwelling waves at the eastern boundary are clearly shown in the September SSH deviation (Figure 1e). The only mechanism for forcing such upwelling waves is the easterly wind between May and September in the central equatorial basin (Figure 2a) (the alongshore wind at the eastern boundary is northward in this season, so it forces downwelling Rossby waves in the northern hemisphere). In the central equatorial ocean the zonal wind becomes westerly between September and November. Downwelling waves forced by this change are observed near the eastern boundary in December's SSH deviation (Figure 1f).

The model results (Figure 3) compare reasonably well with the T/P data (Figure 1) in the northern basins, along the equator, and in the regions off the eastern boundary, but rather poorly in the interior in the southern hemisphere, particularly in the region south of 15°S and west of 85°E. This region is less affected by long Rossby waves radiating from the eastern boundary. The model variability in this region is dominated by a chain of westward propagating waves that appear to be the second baroclinic mode Rossby waves at the annual frequency. It is unclear why such waves, absent in the T/P observations, are generated in the model. Meanwhile the model does not include the ITF, so the generally good agreement between the model and the data in the eastern Indian Ocean appears to indicate that the wind-stress forcing within the Indian Ocean is mainly responsible for Rossby waves radiating from the eastern boundary. The magnitude of the SSH deviations in the southern hemisphere, however, is generally smaller than that in the data. It is not clear at present whether this is due to the lack of ITF.

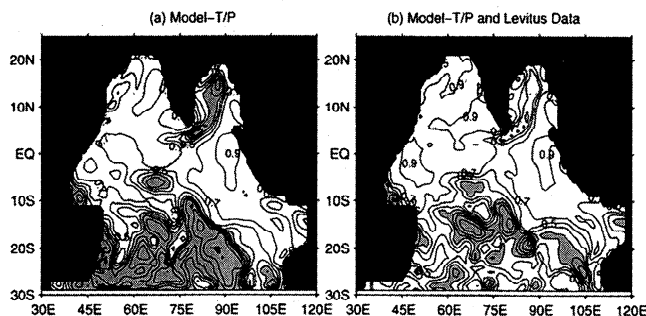


Figure 4. The distribution of correlation coefficient (a) between T/P observation and model results, and (b) between T/P observation and the new field that combines both model SSH and the mixed-layer, temperature-induced SSH. (Contour interval: 0.2; negative correlations are shaded).

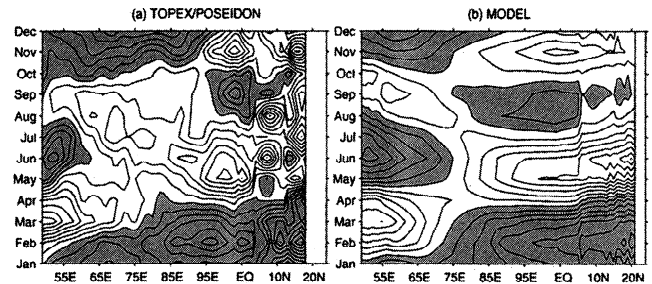


Figure 5. The evolution of the SSH deviation along the equator and the northeastern boundary, (a) from T/P data and (b) from the model. (Contour interval: 1.5 cm; negative SSH deviations are shaded).

The correlation coefficient between the model and T/P observations is shown in Figure 4a. High correlation, ranging from 0.7 to 0.9, is found along the equator, in the southeastern Indian Ocean, and in the northern Indian Ocean but not in the interior of the Bay of Bengal. The southwestern Indian Ocean, a region less affected by Rossby waves, has low correlation. The reason for the poor model–data agreement in those regions is likely due to the lack of thermodynamics in the model (to be discussed below), the open boundary conditions, or the absence of the Indonesian Throughflow.

The seasonal SSH deviation along the equator and along the northeastern boundary is presented in Figure 5 to demonstrate the connection between equatorial and eastern boundary Kelvin waves. It indicates that semi-annual Kelvin waves dominate the seasonal SSH variations along the equator and at the eastern boundary. The propagation of Kelvin waves from the equatorial waveguide to the eastern boundary is quite clear in both data (Figure 5a) and the model (Figure 5b). The less smooth transitions at 5°N are due to a sudden change of the eastern boundary location.

The T/P data (Figure 5a) indicate that Kelvin waves travel across the basin in about 1 to 1.5 months with a phase speed of roughly 1.5 to 2.2 m s⁻¹. This is between the phase speeds of the first and second mode Kelvin waves in the model. At 10°N the longitude–time diagram shows westward propagation of Rossby waves in both the Bay of Bengal and the Arabian Sea (Figure 6a). The phase speed estimated in the Arabian Sea is about -0.17 m s⁻¹, very close to the phase

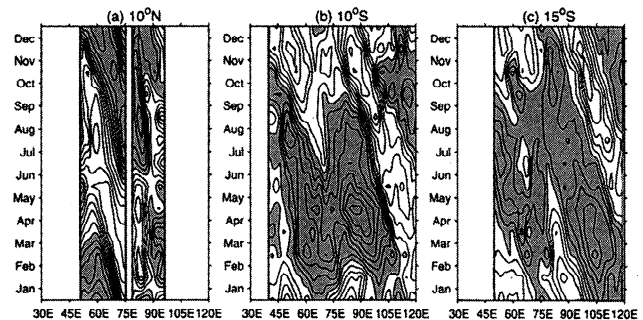


Figure 6. Longitude vs. time diagrams for T/P data at (a) 10°N, (b) 10°S, and (c) 15°S. (Contour interval: 2 cm; negative SSH deviations are shaded).

speed of the first baroclinic mode linear waves. At 10°S (Figure 6b) the westward propagation speed is about -0.14 m s^{-1} , between the first and second mode linear waves. At 15°S (Figure 6c) the phase speed of Rossby waves is about -0.2 m s^{-1} , considerably faster than the first baroclinic mode Rossby waves. In the real ocean the speeds of Kelvin and Rossby waves depend on the local stratification and flow fields.

During the transition from the northeast monsoon to the southwest monsoon, wind speed is minimal in March and April. The latent heat flux in the Bay of Bengal in these two months is reduced to half its annual mean level (from the Comprehensive Ocean-Atmosphere Data Set). The water temperature in the upper 100 meters increases as much as 2°C from below the annual mean in March to almost 1°C higher than the annual mean in April according to the Levitus et al. [1994] climatology (not shown here). The warming continues through the northern spring and summer. The thermal expansion effect in this 100-m water column can cause the SSH change up to 8 cm in the western Arabian Sea and in the central and western Bay of Bengal (not shown). By adding this thermal effect to the model results, the model-T/P correlation in the Bay of Bengal, the Arabian Sea, and the southwestern Indian Ocean is highly improved (Figure 6b).

4. Summary

Our analyses of the SSH data from the TOPEX/POSEIDON altimeter and from a 2.5-layer, reduced gravity model indicate that Kelvin and Rossby waves play dominant roles in the seasonal variation of the sea level in the tropical and subtropical Indian Ocean. The similarity between model and observations is particularly remarkable in regions that are strongly affected by Kelvin waves and radiated/reflected Rossby waves, such as in the equatorial waveguide and in the regions off eastern boundaries. Analyses of surface heat flux and water temperature variation indicate that thermodynamics plays a significant role in the extratropical southwestern Indian Ocean and in the northern Indian Ocean during the spring warming period. The results from a sensitivity test in which equatorial Kelvin waves are dampened suggest that equatorial remote forcing contributes significantly to extratropical seasonal variations, particularly during the southwest monsoon season and in the southeastern Indian Ocean.

Acknowledgments. We thank J. O'Brien and J. Stricherz at Florida State University for providing the surface wind stress data. The paper was written while JY was visiting Goddard Space Flight Center, NASA, where he was supported by the Universities Space Research Association's Goddard Visiting Scientist Program. This research was supported by grant OCE 96-16951 from the National Science Foundation. We thank A. Plueddemann and four

anonymous reviewers for constructive comments. Contribution 9508 from the Woods Hole Oceanographic Institution.

References

- Adamec, D., and J. J. O'Brien, The seasonal upwelling in the Gulf of Guinea due to remote forcing, *J. Phys. Oceanogr.*, **8**, 1050-1060, 1978.
- Clarke, A. J., and X. Liu, Observations and dynamics of semi-annual and annual sea levels near the eastern equatorial Indian Ocean boundary, *J. Phys. Oceanogr.*, **23**, 386-399, 1993.
- Jensen, T. G., Modeling the seasonal undercurrents in the Somali Current system, *J. Geophys. Res.*, **96**, 22,151-22,167, 1991.
- Jensen, T. G., Equatorial variability and resonance in a wind-driven Indian Ocean model, *J. Geophys. Res.*, **98**, 22,533-22,552, 1993.
- Levitus, S., et al., NOAA Atlas NESDIS 1, Washington, D.C., Vols. 1, 2, 3, and 4, U.S. Govt. Printing Office, 1994.
- Lighthill, M. J., Dynamic response of the Indian Ocean to the onset of the southwest monsoon, *Philos. Trans. Roy. Soc. London, Ser. A*, **265**, 45-92, 1969.
- Luther, M. E., and J. J. O'Brien, A model of the seasonal circulation in the Arabian Sea forced by observed winds, *Prog. Oceanogr.*, **14**, 353-385, 1985.
- Luther, M. E., and J. J. O'Brien, Modelling the variability in the Somali Current, in *Mesoscale/Synoptic Coherent Structures in Geophysical Turbulence*, edited by J. C. J. Nihoul and B. M. Jamart, pp. 373-386, Elsevier Science Publ., Amsterdam, 1989.
- McCreary, J. P., P. K. Kundu, and R. L. Molinari, A numerical investigation of dynamics, thermodynamics and mixed-layer processes in the Indian Ocean, *Prog. Oceanogr.*, **31**, 181-244, 1993.
- Perigaud, C., and P. Delecluse, Annual sea level variations in the southern tropical Indian Ocean from Geosat and shallow-water model simulations, *J. Geophys. Res.*, **97**, 20,169-20,178, 1992.
- Potemra, J. T., M. E. Luther, and J. J. O'Brien, The seasonal circulation of the upper ocean in the Bay of Bengal, *J. Geophys. Res.*, **96**, 12,667-12,683, 1991.
- Stricherz, J., D. M. Legler, and J. J. O'Brien, Atlas of Florida State University Indian Ocean Winds for TOGA 1970-1985, The Florida State University, Tallahassee, 250 pp., 1993.
- Yu, L., J. J. O'Brien, and J. Yang, On the remote forcing of the circulation in the Bay of Bengal, *J. Geophys. Res.*, **96**, 20,449-20,454, 1991.

David Adamec and Chester J. Koblinsky, Oceans and Ice Branch, Goddard Space Flight Center, NASA, Greenbelt, MD 20771.

Jiayan Yang, Dept. of Physical Oceanography, Woods Hole Oceanographic Institution, Woods Hole, MA 02543-1541. (e-mail: jyang@whoi.edu)

Lisan Yu, Joint Center for Earth System Sciences and Department of Meteorology, University of Maryland, College Park, MD 20742.

(Received November 9, 1997;
accepted April 8, 1998.)